

Supporting information

Enhanced Ideal Strength in the Thermoelectric Half-Heusler TiNiSn by Sub-Structure Engineering

Guodong Li ^{†,‡}, Qi An ^{⊥,||}, Umut Aydemir [‡], William A. Goddard III [⊥], Max Wood [‡], Pengcheng Zhai [†], Qingjie Zhang ^{*,†}, and G. Jeffrey Snyder ^{*,‡,§}

[†]State Key Laboratory of Advanced Technology for Materials Synthesis and Processing, Wuhan University of Technology, Wuhan 430070, China.

[‡]Department of Materials Science and Engineering, Northwestern University, Evanston, Illinois 60208, USA.

[⊥]Materials and Process Simulation Center, California Institute of Technology, Pasadena, California 91125, USA.

^{||}Materials Science and Engineering, University of Nevada, Reno, Reno, Nevada, 89557, USA.

[§]ITMO University, St. Petersburg, Russia

*Corresponding authors: jeff.snyder@northwestern.edu; zhangqj@whut.edu.cn

Uniaxial tension induced failure mechanism of TiNiSn

a. Tensile stress–strain relationship

To understand the tensile mechanics of TiNiSn, we examined the uniaxial tensile ideal strength at 0 K along different directions, as shown in Figure S1 and Table S1. Tension along [111] direction shows the lowest ideal tensile strength of 20.73 GPa, which is still much higher than that of CoSb₃ (12.9 GPa)¹ and Mg₂Si (5.63 GPa)², demonstrating the excellent mechanical behavior of TiNiSn compared to other TE materials. At small tensile strains (less than 0.05), the stress linearly increases along all tensile directions, and the nonlinear stress response is observed at larger strain until the ideal strength, indicating that the structure is strongly resistant to the tensile deformations. After reaching the maximum tensile stress, the curve starts to fall, corresponding to a ‘plastic’ process. Especially for tension along [100] direction, it shows such a strong yielding process from strain 0.335 to 0.661. However, the stress suddenly drops at the fracture strain, indicating the structure can’t resist the tensile deformation any more, leading to the failure of TiNiSn.

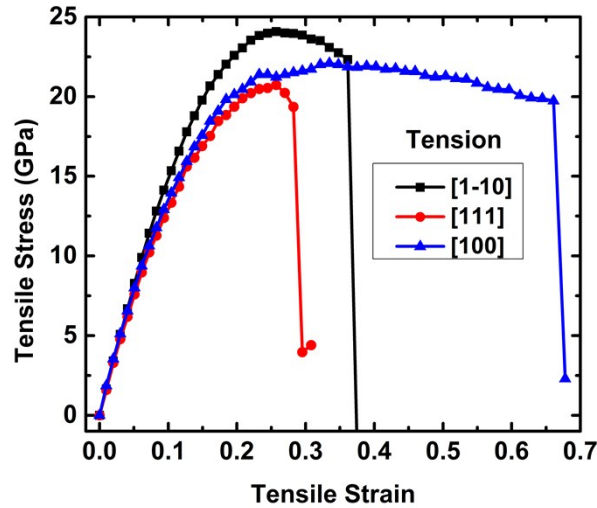


Figure S1. Calculated stress vs. strain of TiNiSn under different directions of uniaxial tension loads.

Table S1. The ideal strength and fracture strain of TiNiSn under uniaxial tension loads.

Mechanics	Tension		
	[100]	[1-10]	[111]
Ideal strength (GPa)	22.09	24.09	20.73
Failure strain	0.678	0.375	0.295

b. Structure and bonding analysis of TiNiSn under tensile loads

In order to obtain the atomistic understanding of the tensile failure of TiNiSn, we extracted the atomic configurations and the typical bond lengths along all three tensile directions. Figure S2 shows the structural changes at various strains along the [111] tensile direction. All the bonds are stretched continuously until the tensile strain of 0.257 corresponding to the ideal tensile strength, as shown in Figure S2(a). As the tensile strain increases to 0.282, the atomic structure further deforms as shown in Figure S2(b). Note that the tensile stress decreases from 20.73 GPa to 19.35 GPa, indicating bonds soften even though they have not broken yet. However, at the strain of 0.295, the Ni2–Ti3, Ti9–Sn1, and Ni1–Sn8 bonds are fully broken, releasing the tensile stress to 3.95 GPa, suggesting the structural collapse. These typical bond lengths with the increasing tensile strain are plotted in Figure S2(d). At small strains, all the bonds are stretched uniformly, corresponding to elastic deformation as shown in Figure S1. With the further increased strain, the Ni2–Ti3 bond is stretched much faster than the other bonds, indicating the Ni2–Ti3 bond softens before the other bonds. Prior to the failure strain of 0.295, the Ni2–Ti3, Ti9–Sn1, and Ti1–Sn8 bonds are stretched from 2.58, 2.97 and 2.58 Å to 3.49, 3.23, and 3.11 Å, with an increase of 35.27%, 8.75%, and 20.54%, respectively. The Ni2–Ti3 bond shows a much higher stretching ratio than that of Ti9–Sn1 and Ni1–Sn8 bonds, suggesting a highly weakened Ni2–Ti3 bond before failure. But the rigidity of the TiSn framework slightly decreases because of the lowest stretching ratio (8.75%) of Ti9–Sn1 bond. However, the Ti9–Sn1 bond length sharply increases to 4.64 Å at the fracture strain of 0.295, indicating bond breakage and the collapse of TiSn framework, leading to the tensile fracture of TiNiSn.

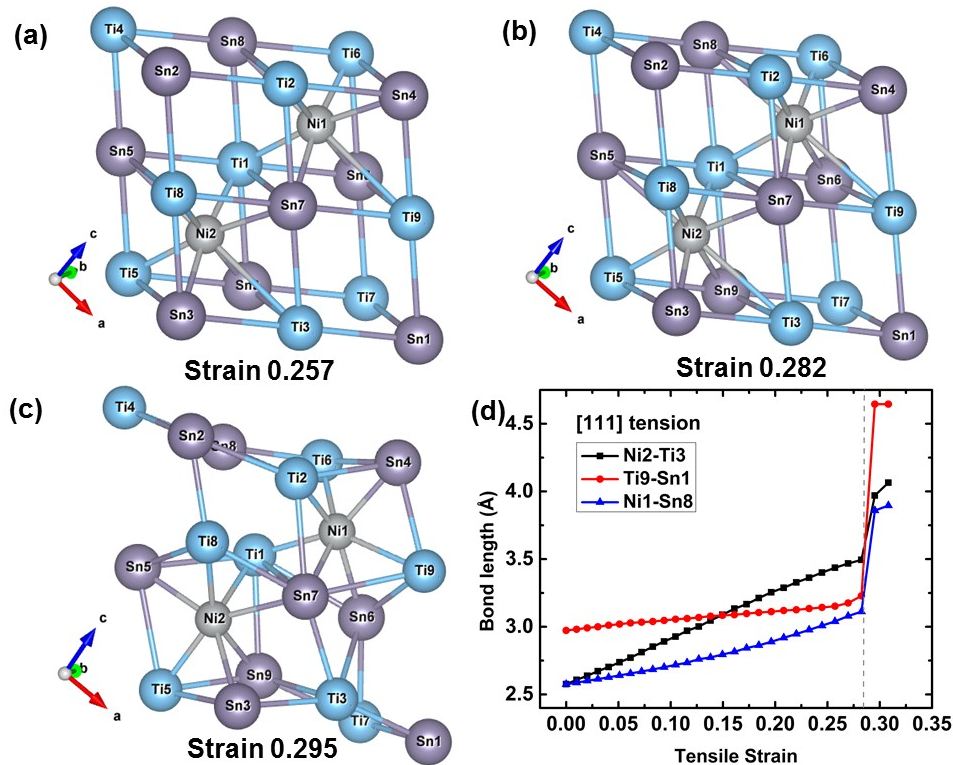


Figure S2. The atomic structures along the [111] tension: (a) structure at 0.257 strain corresponding to the ideal strength, (b) structure at 0.282 strain before failure strain, (c) structure at failure strain 0.295. (d) The average bond lengths (Ni2–Ti3, Ti9–Sn1, and Ni1–Sn8 bonds) with the increasing tensile strain along the [111] tension. The gray dashed line represents the strain just before failure.

The structural changes and the average bond lengths (Ni1–Ti4, Ti5–Sn9, and Ni2–Sn4 bonds) at various strains for [1-10] tension are shown in Figure S3. At a strain of 0.257 corresponding to the maximum stress of 24.09 GPa, the TiSn framework can't remain cubic as shown in Figure S3(a) but the structure exhibits the maximal resistance on external deformations. As the strain increases to 0.361, the TiSn framework deforms continually but the structural rigidity gradually softens because the stress is decreased. At the fracture strain of 0.375, the TiSn framework can't resist tensile deformations and collapse as shown in Figure S3(c), with the stress steeply decreasing from 22.33 GPa to -2.02 GPa. The typical bond lengths of Ni1–Ti4, Ti5–Sn9, and Ni2–Sn4 with the tensile strain are plotted in Figure S3(d). With the increased strain from 0 to 0.361, the Ni1–Ti4 bond is stretched much faster than the other bonds, indicating the more softening effects of Ni1–Ti4 bond than the other bonds. Prior to the failure strain of 0.295, the Ni1–Ti4, Ti5–Sn9, and Ni2–Sn4 bonds are stretched from 2.58, 2.97 and 2.58 Å to 3.27, 3.50, and 3.11 Å, with an increase of 26.74%, 17.85%, and 20.54%, respectively. The Ni1–Ti4 bond shows a much higher stretching ratio than that of Ti5–Sn9, and Ni2–Sn4 bonds, suggesting that

the Ni1–Ti4 bond softens before the other bonds. However, the breakage of Ti5–Sn9 bond (6.42 Å) a strain of 0.375 leads to the collapse of the TiSn framework and the tensile fracture of TiNiSn.

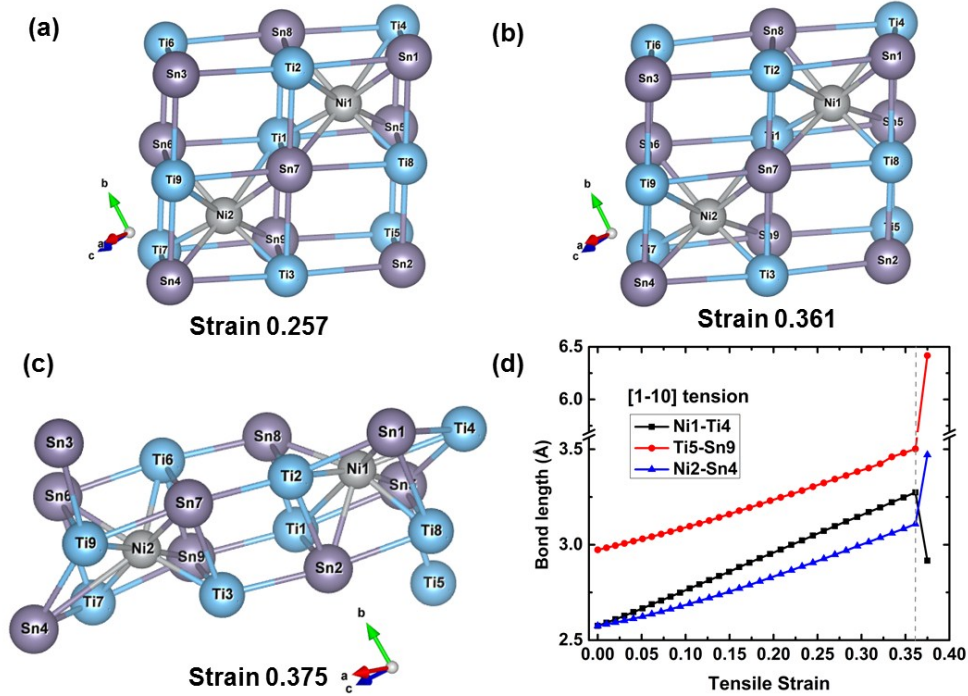


Figure S3. The atomic structures along the [1-10] tension: (a) structure at 0.257 strain corresponding to the ideal strength, (b) structure at 0.361 strain before failure strain, (c) structure at failure strain 0.375. (d) The average bond lengths (Ni1–Ti4, Ti5–Sn9, and Ni2–Sn4 bonds) with the increasing tensile strain along the [1-10] tension. The gray dashed line represents the strain just before failure.

The structural snapshots and the average bond lengths (Ni2–Sn3, Ni2–Ti7, Ti6–Sn3, and Ti7–Sn3 bonds) at various strains for the [100] tension are shown in Figure S4. At the 0.335 strain, the structure deforms uniformly and the TiSn framework changes to a rectangular shape as shown in Figure S4(a). As the strain increases to 0.661, the TiSn framework still remains rectangular in shape while the rigidity of TiSn framework is highly softened because of the rapid increase of Ti6–Sn3 bond length (from 2.97 to 4.94 Å). Meanwhile, the Ni2–Sn3 and Ni2–Ti7 bonds are uniformly stretched (Figure S4(d)), indicating the structure uniformly resists the deformation, which well explains the larger plastic deformation from strain 0.335 to 0.661 as shown in Figure S1. Finally, the further deformation deconstructs the TiSn framework and causes the structural collapse at a fracture strain of 0.678 as shown in Figure S4(c). The typical bond lengths of Ni2–Sn3, Ni2–Ti7, Ti6–Sn3, and Ti7–Sn3 bonds show linear changes with the tensile strain until the fracture strain as plotted in Figure S4(d), which verifies that the structure

uniformly resists tensile deformation. The Ni2–Sn3 bond is linearly stretched from 2.97 to 4.94 Å with a stretching ratio of 66.33%, meanwhile the Ti7–Sn3 bond shrinks from 2.97 to 2.69 Å with a shrinking ratio of 9.43%. The Ni2–Sn3 and Ni2–Ti7 bonds are simultaneously stretched from 2.58 to 3.12 Å with a stretching ratio of 20.93%. The breakage of Ni2–Sn3 and Ni2–Ti7 bonds (4.61 and 5.51 Å) can't maintain structural uniformity, leading to the collapse of TiSn framework.

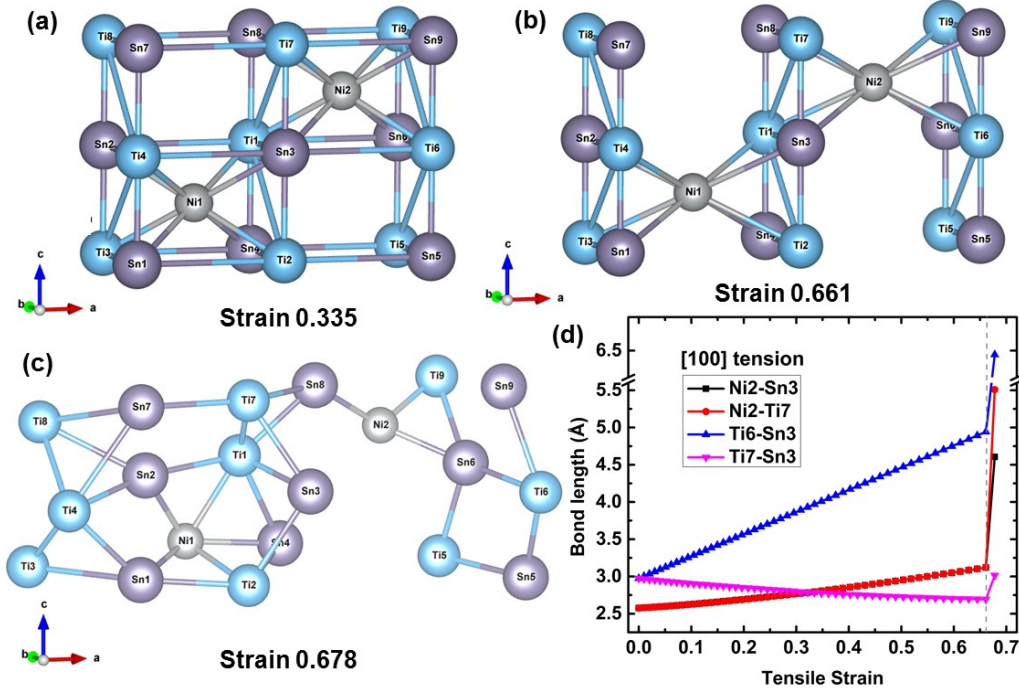


Figure S4. The atomic structures along the [100] tension: (a) structure at 0.335 strain corresponding to the ideal strength, (b) structure at 0.661 strain before failure strain, (c) structure at failure strain 0.678. (d) The average bond lengths (Ni2–Sn3, Ni2–Ti7, Ti6–Sn3, and Ti7–Sn3 bonds) with the increasing tensile strain along the [100] tension. The gray dashed line represents the strain just before failure.

The effect of the random structure on mechanics of $\text{Ti}_{0.5}\text{Hf}_{0.5}\text{NiSn}$

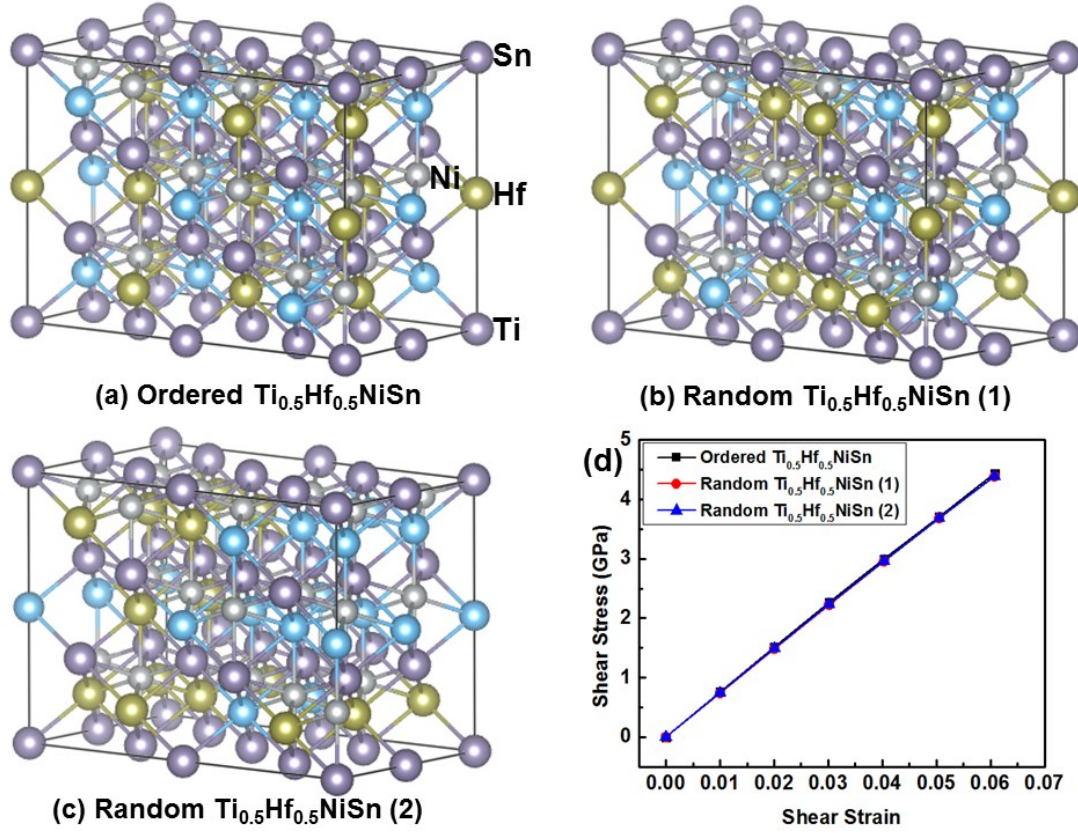


Figure S5. (a) The ordered structure of $\text{Ti}_{0.5}\text{Hf}_{0.5}\text{NiSn}$ alloy along the (111)/<1-10> slip system, (b) A special random structure of $\text{Ti}_{0.5}\text{Hf}_{0.5}\text{NiSn}$ alloy along the (111)/<1-10> slip system, (c) Another special random structure of $\text{Ti}_{0.5}\text{Hf}_{0.5}\text{NiSn}$ alloy along the (111)/<1-10> slip system, (d) Calculated shear stress vs. strain of $\text{Ti}_{0.5}\text{Hf}_{0.5}\text{NiSn}$ alloy under different structures.

REFERENCES

- (1) Li, G. D.; An, Q.; Li, W. J.; Goddard, W. A.; Zhai, P. C.; Zhang, Q. J.; Snyder, G. J., Brittle Failure Mechanism in Thermoelectric Skutterudite CoSb₃. *Chem. Mater.* **2015**, 27, 6329-6336.
- (2) Fan, T. W.; Ke, J. L.; Fu, L.; Tang, B. Y.; Peng, L. M.; Ding, W. J., Ideal Strength of Mg₂X (X = Si, Ge, Sn and Pb) from First-Principles. *J. Magnes. Alloy.* **2013**, 1, 163-168.